Transmission Line Impedance Models Considering Oxygen Transport Limitations in Polymer Electrolyte Membrane Fuel Cells

Touhami S., J. Mainka, J. Dillet, S. Ait Hammou Taleb, O. Lottin

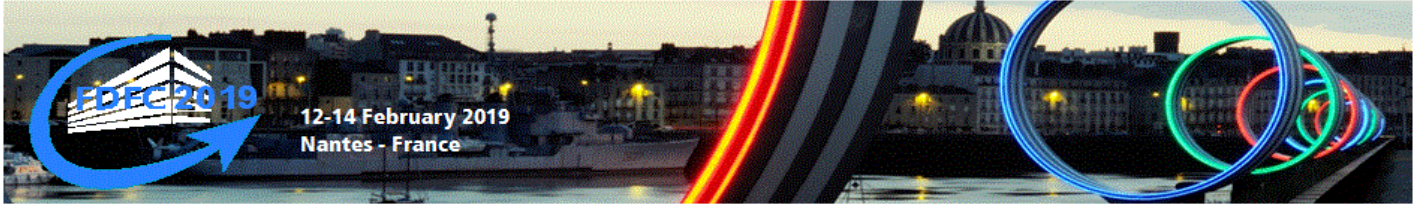

Transmission Line Impedance Models Considering Oxygen Transport Limitations in Polymer Electrolyte Membrane Fuel Cells

S. Touhami, J. Mainka, J. Dillet, S. Ait Hammou Taleb, O. Lottin
LEMTA, UMR CNRS 7563, CNRS/Université de Lorraine, Vandœuvre-lès-Nancy, France.
Salah.Touhami@univ-lorraine.fr

Keywords: PEMFC; Fuel Cell, Electrochemical Impedance Spectroscopy (EIS); porous electrode; Nyquist plot; Electrical Equivalent Circuits (EEC); oxygen transport limitations.

1. Introduction

The main advantage of Electrochemical impedance spectroscopy (EIS) is that phenomena with different time constants can be considered separately in the frequency domain. EIS is generally used to understand the effect of operating conditions on the MEA performance [1], to optimize the electrode structure (ionomer/carbon I/C weight ratio and Pt loading) [2-4], and to analyze its degradation [5-9]. However, the key issue with EIS remains the interpretation of experimental data [10]. On the one hand because of the need of stable operating conditions during the impedance measurements. On the other hand, because impedance models are either based on oversimplified equations or conversely, can sometimes include too many parameters that will reveal correlated. In other words, finding the right level of complexity of the models is not trivial. These models are generally Electrical Equivalent Circuits (EEC) with components such as resistors, capacitors and Warburg-like elements representing the electrochemical half-reactions, as well as charge and mass transport.
In this work, we discuss the validity of different EEC for the interpretation of impedance data measured on two different MEA and cell, as well as in two experimental configurations. In the first case (in operando), the cell is fed with H_2 at the anode and air at the cathode, which allows characterizing reaction kinetics and mass transport losses using a classical Randles EEC [11]. In the second case (blocked electrode), the cell is fed with H_2 at the anode and N_2 at the cathode so that no electrochemical reaction can take place. This allows discriminating between ionic transport limitations in the membrane and the CL. The ionic resistance through the CCL manifests itself through a straight 45° line at high frequencies in the Nyquist plot. This 45° line at high frequencies can also sometimes be observed in operando for certain MEA, and it is typically associated with the ion transport through the porous electrode as a whole [12–15] or within the thin electrolyte film covering the reaction sites [16]. The classical Randles model assuming an interfacial electrode is thus poorly adapted to such spectra and therefore, one will rather use Transmission Line Models (TLM) [17, 18]. Nevertheless, TLM do not usually consider oxygen transport limitations. In order to solve this shortcoming, we studied cathode EEC based on TLM representations that take oxygen transport limitations into account and defined clearly the conditions where they must be used, rather than Randles EEC.

2. Experimental

The experimental data used for this work were obtained using two distinct cells showing significantly different behavior in terms of high frequency impedance.

Cell A: In this configuration, the MEA (H400E) were purchased from SolviCore GmbH & Co. KG. The cathode Pt loading is estimated to be close to 0.4 $mgPt.cm^{-2}$, the exact value being not disclosed by the manufacturer. 235 µm thick gas diffusion layers (GDL) coated with a microporous layer (MPL) (SGL 24BC by SGL Carbon) were used on the anode and cathode sides. The 19.6 cm^2 MEA (98 mm × 20 mm) were inserted between gold coated (1.5 µm) 316L stainless steel plates that ensure current collection and reactant supply through 10 parallel flow channels (1 mm^2) on each side. Both gases flew in the same -vertical- direction (co-flow). The GDL were compressed to 200 µm between the flow field plates, using Teflon gaskets to control their thickness.

Cell B: In the second configuration, the MEA were manufactured in the lab using 25.6 cm^2 (64×40 mm^2) Nafion® XL100 membranes and 7.22 cm^2 (19×38 mm^2) commercial gas diffusion electrodes (GDE) with 0.5 $mg_{Pt}.cm^{-2}$ catalyst layers and 235 µm thick gas diffusion layers (5% PTFE and 80% porosity) coated with Sigracet 29BC MPL. The anode and cathode sides of the MEA were thus strictly identical. The electrodes and the membrane were hot-pressed (T = 135°C, P = 6.2 MPa) 3 minutes and 30 seconds so that the MEA thickness was 410±25 µm. These home-made MEA were used in a cell made of nickel (30 µm) and gold (3 µm) coated brass plates with a single serpentine (1×1 mm^2) flow channel on each side. Both gases flew in counter-flow. The GDL were compressed to 150 µm using Teflon gaskets to control their thickness.
The FC temperature was kept to 60°C with cell A and 70°C with cell B during all experiments. The temperature was controlled thanks to a water circuit. The cathode compartment was supplied with humidified air (70% RH in the first cell and 80% RH in the second cell) with a stoichiometry of 3. The anode compartment was fed with pure hydrogen (70% RH in the first cell and 80% RH in the second cell) with stoichiometries of 1.2 and

1.5 in the first and second cell, respectively. Each new MEA was subjected to a 2 hours conditioning stage consisting of current steps under potentiostatic conditions with voltages set to OCV, 0.6 V and 0.3 V.
Impedance data were measured in galvanostatic mode for H_2/air configuration at 0.5 A.cm^{-2} with a perturbation amplitude limited to 50 mA (peak to peak), with frequencies ranging from 20 mHz to 10 kHz. The potentiostatic spectra were acquired under H_2/N_2 with 0.5 V DC potential and a dynamic perturbation set to 50 mV (peak to peak), for frequencies comprised between 1 Hz and 10 kHz. We paid attention to reduce the impact of the inductance of connecting wires on the system impedance as much as possible.
EI spectra measured with cell B consistently showed a 45° straight line at high frequencies, while that line never appeared with cell A.

3. Randles Circuit and Transmission Line Models

3.1 Electrical Equivalent Circuits

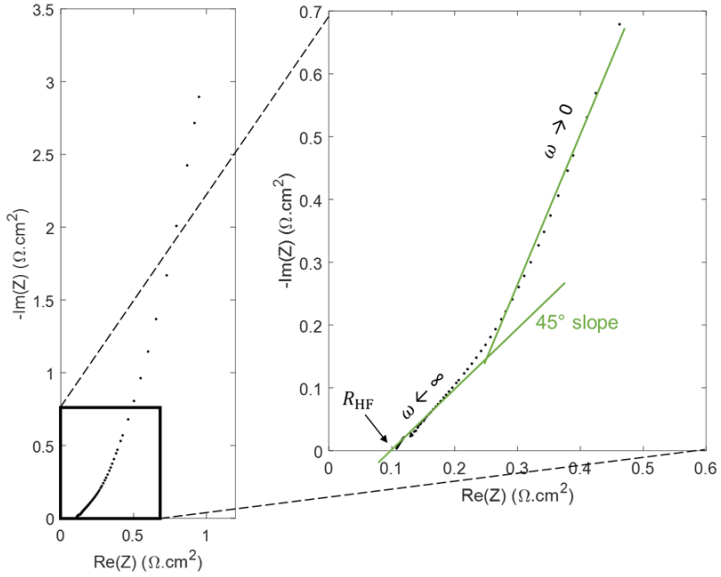

Figure 1: Experimental impedance spectra in a Nyquist diagram for cell B with a blocked electrode (H_2/N_2).

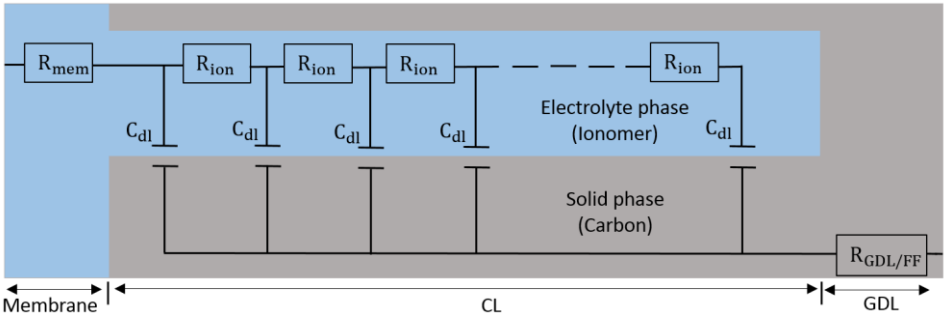

Figure 2: TLM EEC, without oxygen transport limitation, for PEMFC with porous catalyst layer under H_2/N_2.

EIS with a blocked electrode can be used as a complement of in operando characterization to investigate PEMFC cathode structure and transport properties [18]. Figure 1 shows a Nyquist plot of a PEMFC impedance spectrum obtained with a blocked electrode characterized by the straight 45° high frequency line associated with proton conduction losses within the CCL. At low frequencies, the imaginary part of the impedance increases steeply so that it approaches a vertical line associated with a purely capacitive behavior. However, significant deviation from the vertical line can still be observed, which is generally explained by the inhomogeneous distribution of pore radii within the electrode [19]. Keeping apart this deviation, Impedance spectra of blocked electrodes are well represented using TLM, first introduced by de Levie [12, 20]. Figure 2 shows a discretized transmission line, which is based on an assembly of identical pores. Each pore has a length equal to the thickness of the electrode. The ion conducting phase (electrolyte) corresponds to the upper rail of the circuit and the electron conducting phase (carbon and Pt agglomerates) to the lower rail. The resistance of the carbon/Pt agglomerates is usually assumed negligible so that the EEC consists only of a parallel network of double layer capacitances C_{dl} connected via ionomer resistances R_{ion}. In addition, the equivalent circuit often includes an ionic resistance R_{mem} standing for the membrane and an electronic resistance R_{GDL+FF} accounting for the Flow Field (FF) plates, GDL and possibly other contact resistances.

Ultimately, the global impedance of the cell can be written as [3]:

$$Z_{Cell}(\omega) = R_{HF} + Z_{TLM}(\omega) = R_{HF} + \sqrt{\frac{R_{ion}}{i\omega C_{dl}}}\coth\left(\sqrt{i\omega R_{ion} C_{dl}}\right) \quad (1)$$

Where the high frequency resistance is defined as $R_{HF} = R_{mem} + R_{GDL+FF}$. ω is the angular frequency and i the imaginary unit. Equation (1) can be simplified in the high frequency domain, considering that:

$$\lim_{\omega\to\infty}(Z_{TLM}) = \sqrt{\frac{R_{ion}}{i\omega C_{dl}}} \quad (2)$$

And in the low frequency domain:

$$\lim_{\omega\to 0}(Z_{TLM}) = \frac{R_{ion}}{3} + \frac{1}{i\omega C_{dl}} \quad (3)$$

Therefore, R_{ct} and R_{ion} can be easily estimated from the profile of the Nyquist plots. The high-frequency resistance R_{HF} is given by the intersection of the impedance with the x-axis and the intersection between the low-frequency line and the x-axis is $R_{ion}/3 + R_{HF}$, as shown in Figure 1. The ionic resistance R_{ion} plays an important role in the electrochemical behavior of PEMFC cathode, although the main contribution to performance losses is due to the charge transfer resistance R_{ct}. R_{ct} and the double layer capacitance C_{dl}, are the two main parameters characterizing the ORR kinetics. To study their impact on the FC impedance, we performed in operando EIS (H_2/air) with both cells: Figure 3 (top) shows the Nyquist plot of impedance data measured with cell A. This impedance spectrum is composed of two intricated loops: the high frequency loop is governed mostly by electrochemical reaction kinetics while the low frequency loop results from oxygen transport. The typical EEC associated with such FC spectra is the Randles circuit, shown in Figure 4. In a more general way, this EEC is commonly used to interpret the impedance of thin electrodes. It is composed of a charge transfer resistance R_{ct} in parallel with a double layer capacitance C_{dl} characterizing the electrochemical reaction, in series with a high-frequency resistance R_{HF}. Finally, a Warburg impedance Z_W connected in series to R_{ct} accounts for oxygen transport limitations.

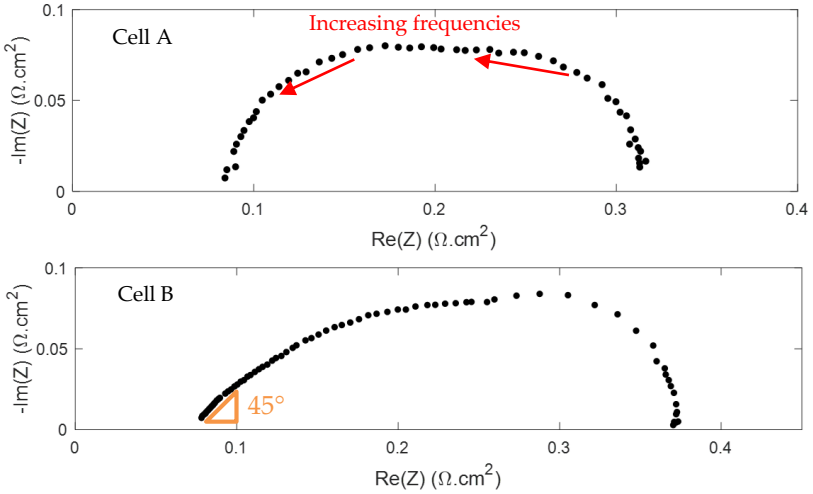

Figure 3: Nyquist diagram of impedance spectra measured in operando (H_2/air) with cells A (top) and B (bottom). The 45° straight line appears only with cell B.

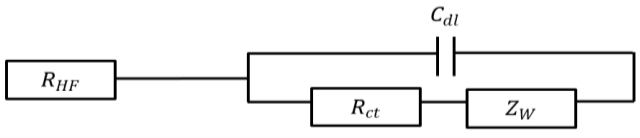

Figure 4: Randles EEC used to model the impedance of PEMFC with thin cathode catalyst layer.

The impedance of this circuit is given by:

$$Z_{Cell}(\omega) = R_{HF} + Z_{Randles}(\omega) = R_{HF} + \left(\frac{1}{R_{ct}+Z_w(\omega)} + i\omega C_{dl}\right)^{-1} \quad (4)$$

With,

$$Z_W(\omega) = \frac{R_d}{\sqrt{i\omega\tau}}\tanh\sqrt{i\omega\tau} \quad (5)$$

Where R_d is the diffusion resistance and τ the time constant of oxygen diffusion through the catalyst layer. The Randles circuit cannot be used to fit and analyze spectra such as that of Figure 3 (bottom), obtained with cell B, because it does not consider the 45° high frequency straight line associated to the ionic resistance through the porous structure of the electrode. This must be done using a TLM-like model. Eikerling and

Kornyshev [16] applied a TLM model (similar to that developed by De Levie for blocked electrodes) to operating FC and calculated the impedance analytically for low currents in the absence of oxygen supply limitations. Later, Makharia et al. [3] proposed a TLM model neglecting oxygen transport limitations and showed that this model and the physical model of Eikerling and Kornyshev were equivalent for low currents. In order to analyze our impedance spectra, we modified the TLM model regarding charge transfer during the ORR -introducing R_{ct} in the model- and mass transfer through the CCL -introducing Warburg elements in series with R_{ct}-as shown in Figure 5. The global impedance of the cell can thus be described as:

$$Z_{Cell}(\omega) = R_{HF} + Z_{CL}(\omega)$$
$$= R_{HF} + \frac{\sqrt{R_{ion}}}{\sqrt{i\omega C_{dl}+(1/(R_{ct}+Z_W(\omega)))}} \coth\left(\sqrt{i\omega R_{ion} C_{dl} + (R_{ion}/(R_{ct}+Z_W(\omega)))}\right) \quad (6)$$

Where $Z_{CL}(\omega)$ stands for the modified expression of the TLM impedance accounting for charge transfer and mass transport through the catalyst layer. Similar expressions were already used in the literature [18] but, to the best of our knowledge, without considering mass transfer.

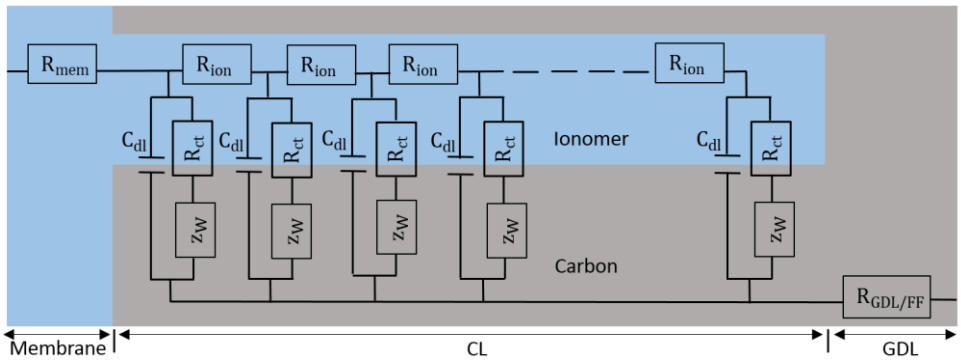

Figure 5: TLM-like EEC accounting for oxygen transport limitations in the CCL for in operando PEMFC.

3.2 Occurrence of the 45° High Frequency Line

To simplify the equations, the oxygen transport limitations (*i.e.* the Warburg impedances) are not taken into account, which can be easily justified by their negligible value at high frequencies. The occurrence of the 45° straight line in EIS Nyquist plots depends thus on the reaction kinetics parameters, R_{ct} and C_{dl}, as well as the ionic resistance R_{ion} and the angular frequency ω. Figure 6 shows impedance spectra computed for different values of R_{ion}, the other parameters remaining unchanged. We can observe a threshold value of the angular frequency above which the 45° straight line is always present; that threshold increases as R_{ion} decreases, so that the 45° straight line may not be observed for CCL with a high ionomer content and/or thin electrodes.

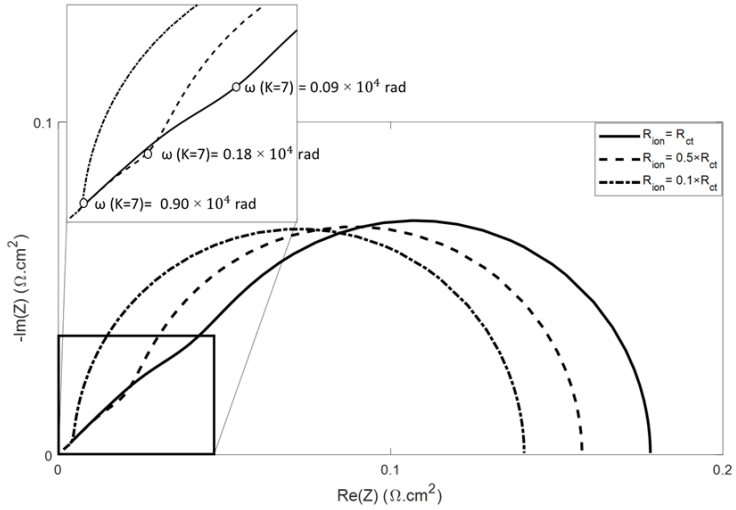

Figure 6: Nyquist plot of impedance spectra simulated using a TLM-like model with different values of the ionic resistance in the CCL. For clarity, the oxygen transport limitations (i.e. the Warburg impedances in Figure 5) are not considered and R_{HF} = 0 Ω.cm². The values of the kinetic parameters $R_{ct} = 0.13\ \Omega.cm^2$ and $C_{dl} = 0.0562\ \Omega/cm^2$ are close to those measured with our cells (Table 1).

To understand the relationship between the ion transport resistance through the CCL and the extent of the 45° line in the Nyquist plot, we need to consider the non-dimensional ratio K between the ionic resistance R_{ion}

and the impedance of the other elements of the branch $Z(R_{ct}||C_{dl})$, characterizing the reaction kinetics. In equation (7), $Z(R_{ct}||C_{dl})$ is a function of the angular frequency ω:

$$K = \frac{R_{ion}}{Z(R_{ct}||C_{dl})} = \frac{R_{ion}}{R_{ct}} + i\omega C_{dl} R_{ion} \quad (7)$$

And,

$$\|K\| = \left[\left(\frac{R_{ion}}{R_{ct}}\right)^2 + (\omega C_{dl} R_{ion})^2\right]^{\frac{1}{2}} \quad (8)$$

If $\|K\| < 1$ at the highest scanning frequency, the 45° straight line will not appear in the Nyquist plot and the shape of the impedance spectra approaches that of usual Randles circuits. If $\|K\|$ is close to one or higher, the influence of ion transport on the impedance spectra will be visible above the threshold value of the angular frequency ω_c. In the example shown in Figure 6, ω_c is reached for $\|K\| \approx 7$, such as:

$$\omega_c \approx \left[\left(\frac{7}{C_{dl} R_{ion}}\right)^2 - \left(\frac{1}{R_{ct} C_{dl}}\right)^2\right]^{\frac{1}{2}} \quad (9)$$

Thus, if ion transport is negligible compared to the reaction kinetics limitations, ω_c could be sufficiently high so that the 45° line is not visible in the Nyquist plot. An important consequence of this result is that the modified TLM model presented in Figure 5 corresponds to a general EEC of FC impedance that can be used as well with volumetric, as with thin CCL, since it tends toward the Randles circuit when R_{ion} is sufficiently low. This can be demonstrated starting from equation (6) and considering the first order Taylor expansion of $\coth x = \frac{1}{x} + \frac{x}{3}$: we have thus $\lim_{x\to 0} \coth x = \frac{1}{x}$ when, $R_{ion} \to 0$, and the modified TLM impedance becomes:

$$\lim_{R_{ion}\to 0} Z_{CL} = \frac{\sqrt{R_{ion}}}{\sqrt{\frac{1}{R_{ct}+Z_W} + i\omega C_{dl}}} \frac{1}{\sqrt{R_{ion}}\sqrt{\frac{1}{R_{ct}+Z_W} + i\omega C_{dl}}} = \frac{1}{\frac{1}{R_{ct}+Z_W} + i\omega C_{dl}} \quad (10)$$

Which corresponds to the cathode catalyst layer resistance $Z_{Randles}$ of the Randles EEC given in equation (4).

3.3 Location of the Main Mass Transfer Resistance

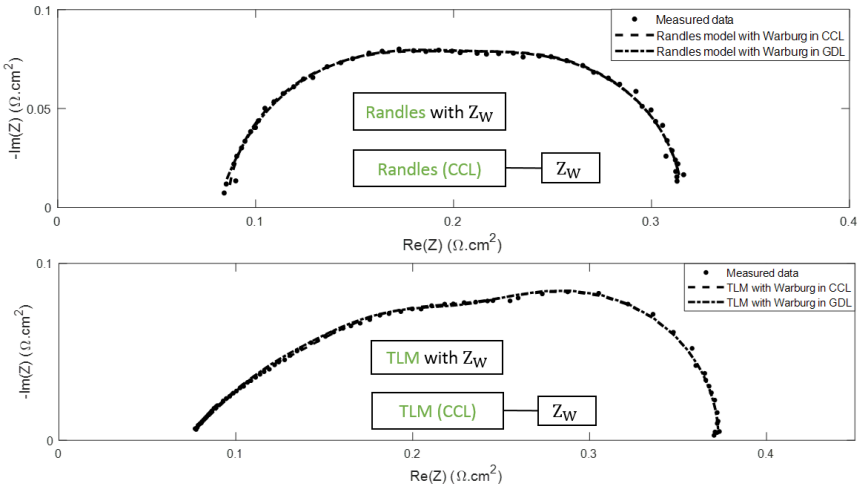

Figure 7: Nyquist diagram of impedance spectra measured in operando (H_2/air), and spectra simulated using a Randles EEC with cell A (top) and using a TLM-like model with cell B (bottom).

We have just shown that the modified TLM model in Figure 5 is equivalent to the usual Randles EEC when the ionic resistance through the catalyst layer is negligible. This leads us to the conclusion that the Warburg impedance in the Randles circuit corresponds to an oxygen transport resistance that is physically located in the catalyst layer, which is inherently in contradiction with the hypothesis of a surface electrode, often put forward with Randles EEC. Since significant mass transfer resistance may appear through the gas diffusion layer, the most appropriate way to take them into account consists in using a modified Randles EEC with the Warburg impedance connected in series to the reaction kinetics parameters R_{ct} and C_{dl}, such as presented in Figure 7 (top). Of course, the same approach can be followed with TLM-like models, using an EEC such as shown in Figure 7 (bottom). It must be noted that both EEC in Figure 7 consider oxygen transport resistance in the GDL or the CCL only, although it would still be possible, at least from a mathematical point of view, to keep Warburg elements in series with the charge transfer resistance R_{ct} (and in parallel with C_{dl}) to account also for oxygen transport resistances through the CCL. Nevertheless, these two mass transfer resistances -through the CCL and in the GDL- would reveal highly correlated. In this work, we thus limited ourselves to four options:

1. Usual Randles EEC (Figure 4) with Warburg impedance in the CCL *vs.* modified Randles EEC with Warburg impedance in series -Figure 8 (top)-, applied to impedance spectra measured with cell A (see the experimental section), *i.e.* without a 45° straight line at high frequencies.
2. TLM-like EEC (Figure 6) with Warburg impedance in the CCL *vs*. TLM-like EEC with Warburg impedance in series -Figure 8 (bottom)-, applied to impedance spectra measured with cell B (see the experimental section), *i.e.* with a 45° straight line at high frequency.

The data and graph in Figure 7 show that both approaches (Warburg elements in the CCL or in series) allow to fit rather well the experimental spectra, with similar standard deviations. This is the case with cell A (Randles EEC) as well as will cell B (TLM-like EEC). The corresponding values of the model parameters are given in Table 1: they show that despite of their ability to fit well the experimental data, both approaches cannot be considered as equivalent since the corresponding values of the kinetic parameters differ up to 40%.

	R_{HF} ($\Omega.cm^2$)	τ (s)	R_d ($\Omega.cm^2$)	R_{ion} ($\Omega.cm^2$)	C_{dl} (F/cm^2)	R_{ct} ($\Omega.cm^2$)
Cell A						
Randles EEC with Z_W in CCL	0.086	0.066	0.097		0.034	0.132
Randles EEC with Z_W in GDL	0.078	0.077	0.135		0.053	0.102
Cell B						
TLM with Z_W in CCL	0.069	0.066	0.122	0.234	0.034	0.108
TLM with Z_W in GDL	0.071	0.073	0.172	0.191	0.057	0.074

Table 1: Estimated parameters starting from the experimental data and models in Figure 7.

4. Conclusions

The main conclusion of this work is that TLM-like EEC modified to consider charge transfer resistance as well as oxygen transport resistance can be used instead of Randles EEC to model PEMFC CCL impedance since they correspond to a more complete representation: the impedance of such TLM-like EEC tends toward that of a Randles EEC when the ion transport resistance through the catalyst layer becomes negligible. Similarly, the occurrence of the 45° straight line at high frequencies depends on the ratio between the ionic resistance and the elements characterizing the reaction kinetics: R_{ct} and C_{dl}. This is the reason why the 45° straight line is always observed with blocked electrodes, but only sometimes during fuel cell operation.

Finally, these considerations lead us to the conclusion that the Warburg impedance in the Randles circuit corresponds to an oxygen transport resistance that is physically located in the catalyst layer, which is in contradiction with the hypothesis of a surface electrode that governs the derivation of the Randles EEC. Assuming that the main oxygen transport limitation is in the GDL would be more consistent with Randles EEC, but this hypothesis means that the Warburg impedance should be connected in series with the charge transfer resistance and double layer capacitance. We have seen that such a modification has a significant impact on the values of the kinetics parameters that can be identified from impedance spectra.

REFERENCES

1. J. Zhang et al., Electrochimica Acta, vol. 52, no 15, p. 5095-5101, 2007.
2. Y. Liu et al., ECS Transactions, Washington, DC, 2007, vol. 11, p. 473-484.
3. R. Makharia, M. F. Mathias, et D. R. Baker, J. Electrochem. Soc., vol. 152, no 5, p. A970, 2005.
4. A.A. Kulikovsky, Electrochim. Acta. 147 (2014) 773–777.
5. S. Shahgaldi, A. Ozden, X. Li, et F. Hamdullahpur, Energy Convers. Manag., vol. 171, p. 1476-1486, sept. 2018.
6. K. H. Lim et al., J. Power Sources, vol. 193, no 2, p. 575-579, sept. 2009.
7. R. Lin, B. Li, Y. P. Hou, et J. M. Ma, Int. J. Hydrog. Energy, vol. 34, no 5, p. 2369-2376, mars 2009.
8. N. Macauley et al., J. Electrochem. Soc., vol. 165, no 6, p. F3148-F3160, 2018.
9. A. C. Fernandes et E. A. Ticianelli, J. Power Sources, vol. 193, no 2, p. 547-554, sept. 2009.
10. M. Chandesris, C. Robin, M. Gerard, Y. Bultel, Electrochem. Acta 180:581-590 (2015).
11. P. M. Gomadam et J. W. Weidner, Int. J. Energy Res., vol. 29, no 12, p. 1133-1151, oct. 2005.
12. R. De Levie, Electrochim. Acta 8 (1963) 751.
13. I.D. Raistrick, Electrochim. Acta 35 (1990) 1579.
14. J.H. Jang, S.M. Oh, J. Electrochem. Soc. 151 (2004) A571.
15. A. Nishikata et al., Corrosion Science 37 (1995) 897.
16. M. Eikerling and A. A. Kornyshev, J. Electroanal. Chem. 475(2):107-123 (1999).
17. Parthasarathy M. Gomadam and John W. Weidner, Int. J. Energy Res; 29:1133–115 (2005).
18. T. Gaumont et al., Int. J. Hydrogen Energy, vol. 42, no 3, p. 1800-1812, 2017.
19. H.-K. Song et al., J. Electrochem. Soc. 151, E102 (2004).
20. R. de Levie, Electrochimica Acta, vol. 9, no 9, p. 1231-1245, sept. 1964.